Autoionization widths by Stieltjes imaging applied to Lanczos pseudospectra

S. Kopelke,[1] K. Gokhberg,[1] L. S. Cederbaum,[1] F. Tarantelli,[2] and V. Averbukh[3]
[1]*Theoretische Chemie, Physikalisch-Chemisches Institut, Universität Heidelberg, Im Neuenheimer Feld 229, D-69120 Heidelberg, Germany*
[2]*Dipartimento di Chimica, Università degli Studi di Perugia and CNR I.S.T.M., Via Elce di Sotto 8, 06123 Perugia, Italy*
[3]*Department of Physics, Imperial College London, South Kensington Campus, London SW7 2AZ, United Kingdom*

(Received 19 August 2010; accepted 14 November 2010; published online 11 January 2011)

Excited states of atoms and molecules lying above the ionization threshold can decay by electron emission in a process commonly known as autoionization. The autoionization widths can be calculated conveniently using Fano formalism and discretized atomic and molecular spectra by a standard procedure referred to as Stieltjes imaging. The Stieltjes imaging procedure requires the use of the full discretized spectrum of the final states of the autoionization, making its use for poly-atomic systems described by high-quality basis sets impractical. Following our previous work on photoionization cross-sections, here we show that also in the case of autoionization widths, the full diagonalization bottleneck can be overcome by the use of Lanczos pseudospectra. We test the proposed method by calculating the well-documented autoionization widths of inner-valence-excited neon and apply the new technique to autoionizing states of hydrofluoric acid and benzene. © *2011 American Institute of Physics*. [doi:10.1063/1.3523982]

I. INTRODUCTION

There are a number of physical phenomena where the decay of an excited electronic state proceeds radiationlessly through the emission of an electron and is driven by electron correlation. The well-known examples are autoionization[1] (AI) and the Auger decay[2] (AD) where intra-atomic electron correlation gives rise to the decay, and interatomic Coulombic decay[3] (ICD) where the decay happens due to the correlation of electrons located on different atoms. By far the most important characteristic of these processes is the decay width. In the lowest order perturbation theory, its calculation involves evaluation of matrix elements containing electronic wave functions of the initial (bound-like) and final (continuum) states of the decay.[4] An efficient way to calculate these wave functions in the case of large atomic or molecular systems is to employ standard quantum chemistry methods which use $\mathcal{L}^2$ Gaussian basis sets. These methods are, of course, useful for calculating the wavefunction of the bound-like decaying state. However, the functions corresponding to the continuum final states are completely delocalized and cannot be represented correctly in $\mathcal{L}^2$ basis, since it does not allow to impose the proper boundary conditions. Thus, in solving the Schrödinger equation for the final states using $\mathcal{L}^2$ basis one obtains a discretized continuum with improper ($\mathcal{L}^2$) normalization. Direct use of these discrete states for calculation of the continuum properties of the system in question is impossible. Nevertheless, the $\mathcal{L}^2$ methods can still be used for calculating the physical quantities involving bound-continuum matrix elements if the so-called Stieltjes imaging technique is used.[5,6] Stieltjes imaging has been orignally developed for $\mathcal{L}^2$ calculation of the total photoionization cross-sections by Langhoff and co-workers[7,8] and first applied to decay width calculation by Hazi.[9]

The Stieltjes method uses the $\mathcal{L}^2$ discretized continuum to calculate the spectral moments of the square of the bound-continuum transition matrix element in question. These moments are later used to construct consecutive approximations to the decay width. We have previously applied Stieltjes imaging to the calculations of atomic AI and ICD widths of atomic dimers[10,11] using the Fano-ADC-Stieltjes method.[12] In this method, the decaying and the final states of the decay were calculated using the *ab initio* method known as algebraic diagrammatic construction (ADC),[13] while the widths were found using the Fano ansatz.[14] However, the standard implementation of the Stieltjes imaging requires full numerical diagonalization of Hamiltonian matrices and is, therefore restricted to atomic or small molecular systems. This drawback of the Stieltjes imaging technique was realized very early on[15] and a few of suggestions as to how it can be overcome exist in the literature.[15–18]

Very recently, we have proposed a general method for Stieltjes imaging application to large dimension problems. Our method[19] is based on applying the Stieltjes imaging procedure to the block-Lanczos pseudospectra[20] instead of the full spectra of the Hamiltonian. The physically sound choice of the initial guess (or initial block) for the iterative Lanczos (or block-Lanczos) procedure can lead to a dramatic reduction of effort required in the combined Lanczos-Stieltjes technique. For example, a converged Lanczos-Stieltjes calculation of the total photoionization cross-section of benzene molecule required a diagonalization of a matrix of the order of 10^3 by 10^3, while the full ADC(2) Hamiltonian dimension used in the calculation was of the order of 10^6 by 10^6.[19] In this

paper we extend the previous work[19] by utilizing the combination of the Fano-ADC-Stieltjes procedure and the Lanczos method to calculate AI rates in molecular systems. We discuss how to optimize the Lanczos diagonalization parameters to obtain a fast convergence of the autoionization width and demonstrate the applicability of the new technique to autoionization of polyatomic systems.

The article is structured as follows: in Sec. II we describe the basic theory of the Stieltjes imaging technique and the Lanczos method. In the subsection on the Lanczos method it is shown how it can be utilized to determine spectral moments and how the physical aspects of the process in question determine its input parameters. Test calculations of the AI widths in Ne and the results for AI the HF and C_6H_6 molecules are presented and discussed in Sec. III. Section IV is devoted to conclusions.

II. THEORY

A. Fano-ADC method

In the method originally proposed by Fano[14] and further developed by Howat *et al.*[22,23] the decay width of an isolated resonance state is given by

$$\Gamma(E) = 2\pi \sum_{\beta} |\langle \phi_d | \hat{H} - E | \chi^{+}_{\beta,E} \rangle|^2 \tag{1}$$

where $|\phi_d\rangle$ stands for the decaying N-electron state and $|\chi^{+}_{\beta,E}\rangle$ for the outgoing energy-normalized N-electron continuum state of energy E, with β enumerating all open channels of the decay. The sum runs over all available final states at energy E, and the relevant width is found by evaluating $\Gamma(E)$ at $E = E_r$ where E_r is the energy of the decaying state corrected for the interaction with continuum. In the calculations presented in this paper we take $E_r \approx E_d$, the energy of the decaying state.

To find $|\phi_d\rangle$, $|\chi^{+}_{\beta,E}\rangle$, and E_r we utilize the algebraic diagrammatic construction (ADC) method for excited states.[24] The Intermediate State Representation (ISR) approach to ADC[25] has been used. This provides explicit schemes by which one can construct the ADC matrix as a Hamiltonian matrix (in what follows, the ADC Hamiltonian) using the basis of the so-called intermediate states. The explicit knowledge of the many-electron basis of the ADC Hamiltonian provided by ISR is essential for the computation of any physical quantity expressed via matrix elements between two eigenstates of the ADC Hamiltonian. Among such applications are, e.g., evaluation of dipole moments, transition dipole moments, or computation of the decay widths of highly excited resonance states.

Within the ISR approach to excited state ADC, the ADC Hamiltonian is constructed in the basis of intermediate states, $|\tilde{\Psi}_J\rangle$. These states are obtained by orthonormalization of the correlated excited states, $|\Psi^0_J\rangle$,

$$\left|\Psi^0_J\right\rangle = \hat{C}_J |\Psi_0\rangle, \tag{2}$$

where $\hat{C}_J$ are physical excitation operators,

$$\hat{C}_J = \{\hat{c}^{\dagger}_a \hat{c}_k; \hat{c}^{\dagger}_a \hat{c}^{\dagger}_b \hat{c}_k \hat{c}_l, a < b, k < l; \cdots\} \tag{3}$$

and the correlated ground state $|\Psi_0\rangle$ is given by the perturbation series

$$|\Psi_0\rangle = \left|\Phi^{HF}_0\right\rangle + \left|\Psi^{(1)}_0\right\rangle + \left|\Psi^{(2)}_0\right\rangle + \cdots \tag{4}$$

$|\Phi^{HF}_0\rangle$ being the Hartree-Fock ground state.

The orthonormalization of the $|\Psi^0_J\rangle$ proceeds in two steps. First, the correlated states belonging to different excitation classes, $[J]$, with $J = 0$ referring to the correlated ground state, $J = ak$ ($[J] = 1$) to its single particle-hole excitations (1h1p), $J = abkl$ ($[J] = 2$) to the 2-hole-2-particle (2h2p) excitations, and so on, are orthogonalized by the Gram-Schmidt procedure to obtain the precursor states, $|\Psi^{\sharp}_J\rangle$. For example, $[J] = 1$ or the 1h1p precursor states are obtained as

$$|\Psi^{\sharp}_{ak}\rangle = \hat{c}^{\dagger}_a \hat{c}_k |\Psi_0\rangle - |\Psi_0\rangle \langle \Psi_0 | \hat{c}^{\dagger}_a \hat{c}_k | \Psi_0 \rangle. \tag{5}$$

Next, symmetric orthonormalization is performed within each excitation class. Taking again 1h1p states as an example, one has

$$|\tilde{\Psi}_{ak}\rangle = \sum_{bl} |\Psi^{\sharp}_{bl}\rangle (\mathbf{S}^{-1/2})_{bl,ak}, \tag{6}$$

where $\mathbf{S}$ is the overlap matrix of the precursor states.

Within the ADC approach, one can construct an hierarchy of approximations, ADC(m), $m = 1, 2, \ldots$ in which the expansion of the Hamiltonian in the intermediate states of successive excitation classes $[J]$ is truncated in accordance with the correlated ground state (4). Performing the orthonormalization procedure of Eqs. (5) and (6) approximately and consistently with the order of the many-body perturbation theory which is used for the construction of the correlated ground state [see Eqs. (4)], one can express the Hamiltonian matrix elements of the type $\langle \tilde{\Psi}_J | H | \tilde{\Psi}_{J'} \rangle$ analytically via the orbital energies and the electron repulsion integrals.

In this work we employ the ADC(2) and the ADC(2)x schemes. ADC(2) uses second order perturbation theory for the correlated ground state and expands the excited states in 1h1p and 2h2p excitation classes. ADC(2) treats the 1h1p-1h1p and 1h1p-2h2p couplings in second and first order, respectively, and neglects the coupling between different 2h2p intermediate states. The extended ADC(2) scheme, or ADC(2)x, take into account the 2h2p-2h2p interactions to first order.

The construction of the ADC(2) and ADC(2)x Hamiltonian, respectively, requires a selection scheme for the 1h1p and 2h2p configurations.[12] We choose the configurations by looking at the open and closed channels of the decay. For AI this procedure is discussed in.[10] Construction of the ADC Hamiltonian matrices requires carrying out restricted Hartree-Fock calculations and transforming the electron repulsion integrals from the atomic orbital basis into the molecular orbital basis. Throughout this work, these tasks are performed using MOLCAS6 quantum chemical program package.[26]

B. Stieltjes imaging technique

To get an idea how the $\mathcal{L}^2$ continuum pseudospectrum can be used to approximate the Γ(E)[6] it is useful to consider the so-called cumulative function $F(E)$ defined according to

the equations

$$F(E) = \int dE' \Gamma(E') \tag{7}$$

$$\Gamma(E) = \frac{dF}{dE}. \tag{8}$$

Using the pseudospectrum one defines a histogram approximation to $F(E)$

$$\tilde{F}(E) = \sum_{n=1}^{k} \gamma_n, \quad \epsilon_k < E < \epsilon_{k+1}, \tag{9}$$

where $\gamma_n = 2\pi |\langle \phi_d | \hat{H} - E | \chi_{\beta,\epsilon_n} \rangle|^2$ and ϵ_k are the discrete spectrum eigenvalues. At the rise points, $E = \epsilon_k$, the cumulative function is approximated by

$$\tilde{F}(E) = \frac{1}{2}\left[\tilde{F}(\epsilon_k^-) + \tilde{F}(\epsilon_k^+)\right] = \sum_{n=1}^{k-1} \gamma_n + \frac{1}{2}\gamma_k. \tag{10}$$

Applying the Stieltjes derivative to the histogram approximation of F(E) leads to an approximation of Γ(E)

$$\tilde{\Gamma} = \frac{\gamma_k + \gamma_{k+1}}{2(\epsilon_{k+1} - \epsilon_k)} \tag{11}$$

having the correct dimensionality. It shows that the normalization constants associated with the eigenfunctions $|\chi_{\beta,\epsilon_k}\rangle$ are determined by the density of eigenvalues representing the continuous spectrum. However, the numerical results of this approximation using the raw pseudospectrum are poor and tend to converge badly when the underlying basis set is improved. In Stieltjes imaging computations the Stieltjes derivative is not applied directly to the continuum pseudospectrum. Instead, one performs a moment analysis to obtain a "smoothed" spectrum.

The smoothed spectrum can be obtained by a procedure proposed by Langhoff.[5,7,8] Langhoff's method relies on the fact that the wavefunction of a discretized continuum can be used to accurately reproduce the spectral moments, M_n, of the width Γ(E)

$$M_n = \langle \phi_d | (\hat{H} - E)^\dagger \hat{H}^n (\hat{H} - E) | \phi_d \rangle. \tag{12}$$

This expression can be evaluated by introducing the resolution of identity spanning the domain of the final states. If the exact discrete $|\varphi_i\rangle$ and continuum $|\chi^+_{\beta,E}\rangle$ functions of the final states of the decay were known then one could write for the moments

$$M_n = \sum_i E_i^n |\langle \phi_d | (\hat{H} - E) | \varphi_i \rangle|^2 + \int_{E_t}^{\infty} E^n |\langle \phi_d | (\hat{H} - E) | \chi^+_{\beta,E} \rangle|^2 dE, \tag{13}$$

where E_t is the ionization threshold, and E_i and E are the energies of the discrete and continuum final states. However, since the decaying state $|\phi_d\rangle$ is usually localized about the part of the system which carries the initial excitation, the exact behavior of $|\chi^+_{\beta,E}\rangle$ far from the system is unimportant for the evaluation of the matrix elements in Eq. (13). Thus, the exact resolution of identity can be replaced by the one constructed with the discretized continuum functions $|\chi_{\beta,\epsilon_j}\rangle$ resulting in the following expression for M_n

$$M_n = \frac{1}{2\pi} \sum_j \epsilon_j^n \gamma_j. \tag{14}$$

Increasing the size of the basis set used to compute the discrete spectrum usually leads to fast convergence of these moments to their true values. On converging the first 2N moments one can use them to find their principal representation, i.e., N values of ϵ_j and γ_j. Unlike their raw pseudospectrum counterparts, these quantities converge fast with the basis and exhibit the desired "smooth" behavior. They are introduced into the formula for the Stieltjes derivative in Eq. (11) to obtain an approximation to Γ(E).

Computational aspects of the Stieltjes imaging procedure can be found in the detailed tutorial,[27] to which we refer the reader for practical information. We mention here only two properties which are of particular interest to the present work. It can be shown that the positive spectral moments of the photoionization matrix element of the hydrogen atom diverge (see Ref. 5 and references therein). Therefore, negative moments have been used traditionally in the Stieltjes imaging calculations. Second, as has been already mentioned in Sec. I, knowledge of all the $|\chi_{\beta,\epsilon_j}\rangle$ is necessary for the spectral moment calculation [see Eq. (14)], which results in the need for the full diagonalization of the final state ADC Hamiltonian matrix. Even for systems composed of few atoms this presents a serious computational bottleneck, and makes the calculations in the case of larger molecular systems outright impossible. Several authors proposed a number of schemes helping to circumvent this difficulty: Nesbet proposed a solution completely bypassing diagonalization of the Hamiltonian matrix.[15] In that work he applied his method to the boron atom, however, we do not know of any application of his method to polyatomic systems. Ivanov and Luzanov mentioned the applicability of Krylov-space diagonalization technique in conjunction with the full configuration interaction approach to a series of problems, including Stieltjes imaging.[16] They, again, applied their method only to atomic systems (helium and beryllium) and we are not aware of applications to larger systems. Ågren, Carravetta and co-workers exploit the iterative solution of the response-type equations to calculate effective spectral moments from a reduced space.[17,18] These authors have applied their method successfully to several diatomic systems (N_2, O_2, CO, NO, and HF) and to H_2O.

Another way to avoid this bottleneck was proposed in Ref. 19 where the ADC *ab initio* method and Stieltjes imaging were applied to the calculation of molecular photoionization cross sections. It has been shown in Ref. 19 that the knowledge of a relatively low-order Lanczos pseudospectrum is sufficient to obtain the converged spectral moments.[20,21] This made possible successful application of the Stieltjes imaging to systems as large as the benzene molecule where the dimension of the final state subspace can easily be of the order of 10^6 and applications to even much larger systems should be possible too. In this paper we show that the Stieltjes procedure in conjunction with the Lanczos diagonalization method can be used also to calculate the widths of autoionization in atomic

and molecular systems within the Fano-ADC formalism.[12] Before we proceed to discuss the details and results of the application of this technique we draw an outline of how to calculate spectral moments with the Lanczos method.

C. Calculating spectral moments with the Lanczos method

Within the Lanczos diagonalization method,[20,21] the Hamiltonian is represented in the basis of the so-called Lanczos states, $|\psi_j\rangle$, which are obtained by the Krylov states, $|\phi_k\rangle$, $k = 1, 2, \ldots, N$,

$$|\phi_k\rangle = \hat{H}^k|\phi_0\rangle, \quad k = 1, 2, \ldots, N \tag{15}$$

by the Gram-Schmidt orthonormalization procedure. The Krylov states are produced by the repeated action of the Hamiltonian on some initial state, ϕ_0 (15) that is usually chosen to have a big overlap with the Hamiltonian eigenstates that are of interest in the given physical problem. The Lanczos states of successive orders can be used to construct a series of approximations to the Hamiltonian. The Nth order Lanczos approximation to $\hat{H}$ is of the form

$$\hat{H}^{(N)} = \sum_{i,j=0}^{N} |\psi_i\rangle\langle\psi_i|\hat{H}|\psi_j\rangle\langle\psi_j|, \tag{16}$$

where $\langle\psi_i|\hat{H}|\psi_j\rangle$ is tridiagonal. The eigenvalues and eigenvectors of the operator $\hat{H}^{(N)}$ form Lanczos pseudospectrum. With increasing N, the Lanczos pseudospectrum becomes a successively better approximation to the spectrum of $\hat{H}$. A generalization of the Lanczos technique to the case of a set of initial states, $|\phi_0^m\rangle$, is called block-Lanczos method.[20,21,28]

The Lanczos (block-Lanczos) method is useful not only for diagonalizing Hamiltonian matrices of large dimensions, but also for the approximate representation of the functions of the Hamiltonian[28] as well as for approximate solutions of the time-dependent Schrödinger equation.[29] The Lanczos technique can also be used for the calculation of the spectral moments of the type of (12).[28] To this end, the original Hamiltonian has to be substituted by its Lanczos representation

$$\begin{aligned} M_n &= \langle\Psi_d|(\hat{H} - E)^\dagger \hat{H}^n (\hat{H} - E)|\Psi_d\rangle \\ &\approx \langle\Psi_d|(\hat{H} - E)^\dagger (\hat{H}^{(N)})^n (\hat{H} - E)|\Psi_d\rangle \qquad (17) \\ &= \sum_{i=0}^{N} \left(E_i^{(N)}\right)^n \left|\langle\Psi_d|(\hat{H} - E)\right|\chi_i^{(N)}\rangle\Big|^2 \qquad (18) \end{aligned}$$

where $\chi_i^{(N)}$ are the eigenfunctions of $\hat{H}^{(N)}$ and $E_i^{(N)}$ their eigenvalues, while $(\hat{H} - E)$ is the operator coupling the initial to the final state of the decay. While the non-negative moments of the order $0 \le n \le 2N$ can be calculated exactly by (18) with the appropriate choice of the initial state (or block of states),[28] the negative moments required for the Stieltjes imaging can be calculated only approximately.

Since the Lanczos (block-Lanczos) algorithm approximates most effectively the $\hat{H}$ eigenstate subspace spanned by the starting vector (or vectors), one has to consider the physical properties of the system when choosing the initial guess. In the case of AI decay width, for example, the final states of the process that we wish to resolve are of 1h1p type. Thus, those states are mainly described by 1h1p configurations and we would like the Lanczos method to converge most effectively to the true 1h1p eigenstates. Therefore, we compose our starting vectors for the block-Lanczos iterations of the 1h1p ADC intermediate states.

III. ATOMIC AND MOLECULAR AUTOIONIZATION WIDTHS BY STIELTJES IMAGING APPLIED TO THE LANCZOS PSEUDOSPECTRUM OF THE ADC HAMILTONIAN

In order to test the proposed method we applied it to the calculation of AI widths in three systems: Neon atom (Ne), hydrofluoric acid molecule (HF) and benzene molecule (C_6H_6). The autoionization process can set in when an inner-subshell electron is promoted into a vacant orbital. If the energy of this excitation lies above the ionization threshold of the system in question, it can decay by emitting an electron. The final state of this decay consists of the corresponding ion in its ground or excited state and a free electron in a continuum state. We started our investigation with Ne because it has been subject of several theoretical and experimental investigations[10,30] and can be regarded as a reference system.

Consider first autoionization in Ne. The electronic configuration of the ground state of Ne is (He)$2s^2 2p^6$. Autoionizing states of Ne can be obtained by inner-valence excitation, e.g., by promoting the $2s$ electron into the unoccupied $3p$ or higher-energy orbital. In the final state of the autoionization there will be a hole in a $2p$ orbital and an electron in the continuum. All other channels, leading to the shake-up or doubly ionized states of Ne, are closed. Thus, to get a reasonable approximation for the decaying $(2s)^{-1}3p$ state of Ne it is necessary to include all 1h1p configurations into the Hamiltonian of the initial states which have a hole in a $2s$ orbital. To improve the description all 2h2p configurations with one hole in the $2s$ orbital and another one in either the $2s$ or $2p$ orbitals are also included. The energetically accessible configurations form the Hamiltonian matrix of the final state of the decay. In this we therefore include all 1h1p configurations with a hole in a $2p$ orbital. To improve the final state description we additionally include all 2h2p configurations with two holes in $2p$ orbitals.

The calculations for Ne were carried out with the cc-aug-pCVTZ Gaussian basis set[32] augmented with $4s2p2d$ continuum-like diffuse Gaussians.[33] Since by construction the decaying state lies near the lower spectral boundary, it can be easily computed to any degree of precision by the Davidson diagonalization method.[34] The numerically determined energy of the $(2s)^{-1}(3p)$ resonance of 45.3 eV is close to the literature value of 45.54 eV.[10,30] The Hamiltonian matrix obtained by the ADC(2)x method has dimension 5500. The final states were obtained either by fully diagonalizing the matrix or by applying the block Lanczos method. The predominantly 1h1p character of the final states of the AI of Ne allows us to conclude that the best starting block are all the 1h1p configurations of the final state ADC Hamiltonian. Using this starting block, we performed the Lanczos diagonalization with

TABLE I. AI widths of the $(2s)^{-1}(3p)$ excitation in Ne (Γ) obtained using the block-Lanczos pseudospectrum of size N and with the full ADC(2)x spectrum. The experimental decay width is 13 ± 2 meV (Ref. 30).

N	Γ[meV]
250	40.87
350	25.52
400	12.31
500	11.45
600	11.55
1000	11.59
Full (5500)	11.68

5, 7, 8, 10, 12, and 20 block iterations, obtaining 250, 350, 400, 500, 600, and 1000 final states, respectively. The widths computed using the block-Lanczos pseudospectrum as well as the states obtained in full diagonalization are given in Table I. The resulting width calculated with the full spectrum, $\Gamma = 11.68$ meV, was reported previously[10] and is in a very good agreement with experimental value of 13 ± 2 meV.[30] According to Table I, Γ obtained with the Lanczos method converges to the limit value well within the experimental-theoretical discrepancy for a pseudospectrum dimension an order of magnitude smaller than the full spectrum. An even faster convergence is obtained for the decay width of the higher-lying $(2s)^{-1}(5p)$ excitation (see Table II).

As a next step we apply our approach to the AI width of an inner-valence excitation in the HF molecule (ground state electronic configuration $1\sigma^2 2\sigma^2 3\sigma^2 1\pi^4$). We have chosen to concentrate on the HF excited state where a 2σ electron is promoted into the 2π molecular orbital. As shown in Ref. 31, this excitation is higher in energy than the ionization threshold and can thus undergo AI. While the earlier work has described the AI process at the equilibrium geometry of the neutral, we are interested to trace the dependence of the decay width on the interatomic distance. The initial AI state, $|\phi_d\rangle$ (see Eq. (1)), was obtained as the ground state of an ADC Hamiltonian which contains all configurations which are energetically inaccessible in the decay. These are all the 1h1p configurations with a hole in the 2σ molecular orbital and all the 2h2p configurations with one hole in 2σ and another in 2σ, 3σ or 1π. At the equilibrium distance of 0.917 Å, the calculated energy of the decaying state is 38.5 eV above the ground state, in very good agreement with the earlier theoretical value of 38.6 eV.[31] This energy lies below the double ionization potential[3] and also below all shake-up states of the molecule. Consequently, the ADC Hamiltonian of the final states contains all 1h1p configurations with a hole in 3σ or 2π and all 2h2p configurations with two holes in the 3σ and/or 1π orbitals.

TABLE II. AI widths of the $(2s)^{-1}(5p)$ excitation in Ne (Γ) obtained using the block-Lanczos pseudospectrum of size N and with the full ADC(2)x spectrum. The experimental decay width is 2 ± 1 meV (Ref. 30).

N	Γ[meV]
50	4.34
150	3.34
250	2.80
500	2.41
600	2.49
1000	2.61
Full (5500)	2.64

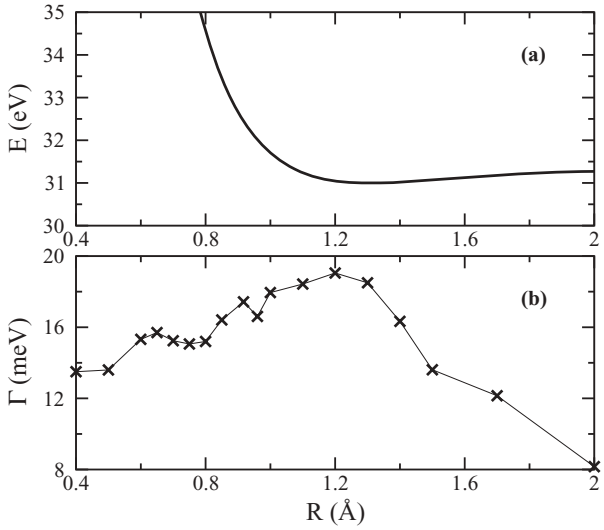

FIG. 1. (a) PEC of the $2\sigma^{-1}2\pi$ HF obtained by adding the MP2 ground state energy to the ADC(2)x excitation energy; (b) the respective AI width as a function of the interatomic distance.

The potential energy curve (PEC) and the AI width of $2\sigma^{-1}2\pi$ HF are shown in Fig. 1. The calculations were done using the uncontracted aug-cc-pVQZ Gaussian basis[32] augmented by $6s6p6d$ continuum-like diffuse Gaussians.[33] The size of the ADC(2)x matrix describing the final states of the AI was 56588. Similarly to the case of Ne, the optimal starting block of the Lanczos diagonalization consists of all 1h1p configurations of the ADC Hamiltonian of the final states subspace. We found that Γ computed by the Lanczos method converges after 50 block-Lanczos iterations or once 5000 Lanczos eigenvectors are obtained. At the equilibrium distance, our AI width $\Gamma = 17.4$ meV is in excellent agreement with the earlier theoretical value of 17 meV obtained by a many-body expansion in conjunction with a discrete basis set approximation.[31] The R-dependence of the decay width has a maximum roughly corresponding to the equilibrium interatomic separation of the decaying state. At shorter distances, the width tends towards the Ne $2s^{-1}3p$ value which is the united atom limit of the molecular AI process. At large internuclear separations, the molecular decay width decreases because of the partial removal of the electronic density from the fluorine atom bearing the inner-valence hole. Each point on the autoionization width curve [Fig. 1b] corresponds to an average of three consecutive Stietjes orders giving the closest results. Numerical inaccuracies inherent to the Stieltjes procedure give rise to a certain degree of roughness in the resulting R-dependence.

To demonstrate the power of the proposed computational method we calculated the width of the $(3e_{2g})^{-1}(3pe_{1u})$ excitations in benzene. At equilibrium geometry, benzene is a planar molecule of D_{6h} symmetry with electronic valence configuration $(2a_{1g})^2(2e_{1u})^4(2e_{2g})^4$

TABLE III. Deacy width, Γ, of $(3e_{2g} \rightarrow 3pe_{1u})$ excitation in benzene for different block-Lanczos matrix sizes. ADC(2) calculation in the aug-cc-pVDZ basis sets.

N	Γ[meV]
26	6.1
130	12.9
260	13.6
780	14.9
1300	15.0

$(3a_{1g})^2(2b_{1u})^2(1b_{2u})^2(3e_{1u})^4(1a_{2u})^2(3e_{2g})^4(1e_{1g})^4$.[35] The subspace used to describe the initial excitation comprises all 1h1p configurations with a hole in the $3e_{2g}$ or $1a_{2u}$ orbital. To account for the electronic correlation in the initial state, we have included in the ADC expansion all 2h2p configurations with holes in the valence space. The huge impact of correlation effects can be seen by considering the energies of $(3e_{2g})^{-1}(3pe_{1u})$ excitations calculated with different subspaces: leaving out just the 2h2p configurations with both holes in the innermost $2a_{1g}$ and $2e_{1u}$ orbitals, leads to a large blue-shift (by more than 10% in our calculations) of the whole energy spectrum. Since the autoionization process of the resonance in question ends up in the cationic state X^2E_{1g} of benzene and with one electron in the continuum, the ADC Hamiltonian of the final states of the decay contains all 1h1p configurations with a hole in the $1e_{1g}$ orbitals and the same complete-valence 2h2p configuration space included in the decaying state ADC Hamiltonian. In the benzene calculations we used the ADC(2) method.

In the benzene calculations, in addition to examining the convergence of the results with the size of the Lanczos subspace, we have also carried out a study of the convergence of the results with the Gaussian basis set. The results of our numerical calculations are given in Tables III, IV, and V. Table III shows the convergence of the computed $(3e_{2g})^{-1}(3pe_{1u})$ decay width with the size of the Lanczos space in calculations using the aug-cc-pVDZ Gaussian basis.[32] The final state ADC matrix was of dimension 435 000. The calculated energy of $(3e_{2g} \rightarrow 3pe_{1u})$ excitation in this basis is 9.52 eV, which is close to the experimental value (9.35 eV[35]) but not converged with respect to the basis sets (see below). The starting subspace for the Lanczos method consists of all the 26 1h1p configurations of the final state ADC Hamiltonian. Table III shows again that the computed value of the AI width converges very fast with the size of the Lanczos matrix. With a Lanczos matrix of dimension only 1300 (which corresponds to 50 iterations with the taken block size of 26) the width is converged within 1%. This confirms that the method provides an extremely practical approach to the calculation of AI widths in molecules.

TABLE IV. Energy and decay width of the $(3e_{2g} \rightarrow 3pe_{1u})$ excitation in benzene calculated using augmented cc-pVDZ basis sets.

Basis	E[eV]	Γ[meV]
aug-cc-pVDZ	9.52	15.0
aug-cc-pVDZ(+1)	9.36	10.8
aug-cc-pVDZ(+2)	9.42	9.3
aug-cc-pVDZ(+3)	9.45	9.1

TABLE V. Energy and decay width of the $(3e_{2g})^{-1}(3pe_{1u})$ excitation in benzene calculated using augmented cc-pVTZ basis sets.

Basis	E[eV]	Γ[meV]
aug-cc-pVTZ	9.66	6.5
aug-cc-pVTZ(+1)	9.61	7.3
aug-cc-pVTZ(+2)	9.61	7.1
aug-cc-pVTZ(+3)	9.61	7.0

In order to assess the reliability of our approximations for the excitation energy and the AI width, we improved the basis sets used until convergence emerged. Table IV shows energies and widths for the $(3e_{2g})^{-1}(3pe_{1u})$ excitation using augmented cc-pVDZ basis sets increasing in size, where (+n), n = 1, 2, 3 means that that the aug-cc-pVDZ basis sets are augmented by n *s*, *p* and *d* Gaussians with continuum-like exponents[33] centered on the C and H atoms. Obviously, the energy of the initial excitation is reasonably well described by all basis sets, converging to 9.45 eV. The width is however greatly sensitive to the basis: the calculated value drops by a third as soon as continuum-like functions are added, although it appears to be relatively more stable with respect to the number of diffuse functions. Increasing the parent basis set from aug-cc-pVDZ to aug-cc-pVTZ (see Table V) also induces a marked variation in the computed Γ, which however becomes less pronounced when continuum-like functions are added. As a result the computed AI width appears to converge to a value of about 7 meV. For the largest basis set used [aug-cc-pVTZ(+3)], the value of the decay width stabilizes at 7.0 meV after 45 block Lanczos iterations (at the Lanczos pseudospectrum dimension of 3600). We emphasize again that studies like the present one would be impossible without exploiting the convergence properties of the Lanczos pseudospectrum: the size of the benzene final state Hamiltonian matrix for the aug-cc-pVTZ(+n) basis sets is of the order of 10^6, clearly not amenable to full diagonalization.

IV. CONCLUSIONS

We have presented an effective scheme to calculate AI rates which overcomes the full diagonalization bottleneck of the standard moment theory approach. Our scheme utilizes the block-Lanczos method to approximate the spectrum of the final states of the decay. Although we find it particularly convenient to use the ADC method for the representation of the many-electron Hamiltonian, the proposed method is completely general and independent of the *ab initio* method employed. We have demonstrated that one can use the block-Lanczos method very effectively to calculate AI rates in atomic and molecular systems, since converged decay widths can be obtained with matrices orders of magnitude smaller than the size of the full spectrum. This permits the successful application of our method to polyatomic systems. In the AI process of the type that we considered, the definition of the bound-like state ϕ_d [see Eq. (1)] was dictated by clear physical principles. In the problems where such a definition

becomes problematic, other methods, such as complex scaling[36] become more appropriate.

We have tested the applicability of our approach by computing AI decay rates for autoionizing states in Ne, HF, and benzene. The results obtained for Ne show how fast the Lanczos results converge to the numbers obtained with the full spectrum and that the scheme delivers results in good agreement with values from the literature. In the case of HF we show that the method is fast enough, such that we can easily determine the width as a function of the inter-nuclear distance and, finally, the application to benzene demonstrates the applicability of our method to larger molecules.

ACKNOWLEDGMENTS

V.A. would like to thank Professor Carravetta for bringing to his attention some of the relevant earlier works.[17,18] Financial support of the DFG is acknowledged. S.K. acknowledges financial support by the *Graduiertenkolleg* of the Interdisciplinary Center for Scientific Computing (IWR) of the University of Heidelberg. V.A. would like to acknowledge the financial support of the EPSRC through the Career Acceleration Fellowship (Grant PHQL_P21289). F.T. acknowledges financial support from the Italian MIUR through PRIN grant n. 2008KJX4SN_003.

[1] *Autoionization*, edited by A. Temkin (Plenum, NY, 1985).
[2] P. Auger, J. Phys. Radium **6**, 205 (1925).
[3] L. S. Cederbaum, J. Zobeley, and F. Tarantelli, Phys. Rev. Lett. **79**, 4778 (1997).
[4] G. Wentzel, Z. Phys. **43**, 524 (1927).
[5] P. W. Langhoff, in *Electron-Molecule and Photon-Molecule Collisions* edited by T. Rescigno, V. McKoy, and B. Schneider (Plenum, New York, 1979).
[6] A. U. Hazi, in *Electron-Molecule and Photon-Molecule Collisions*, edited by T. Rescigno, V. McKoy, and B. Schneider (Plenum, New York, 1979).
[7] P. W. Langhoff, Chem. Phys. Lett. **22**, 60 (1973).
[8] P. W. Langhoff, C. T. Corcoran, J. Sims, F. Weinhold, and R. M. Glover Phys. Rev. A **14**, 1042 (1976).
[9] A. U. Hazi, J. Phys. B **11**, L259 (1978); A. U. Hazi, T. N. Rescigno, and and M. Kurilla, Phys. Rev. A **23**, 1089 (1981); A. U. Hazi, A. E. Orel, and and T. N. Rescigno, Phys. Rev. Lett. **46**, 918 (1981); B. L. Whitten and A. U. Hazi, Phys. Rev. A **33**, 1039 (1986).
[10] K. Gokhberg, V. Averbukh, and L. S. Cederbaum, J. Chem. Phys. **126**, 154107 (2007).
[11] V. Averbukh, I. B. Müller, and L. S. Cederbaum, Phys. Rev. Lett. **93**, 263002 (2004).
[12] V. Averbukh and L. S. Cederbaum, J. Chem. Phys. **123**, 204107 (2005).
[13] J. Schirmer, L. S. Cederbaum and O.Walter, Phys. Rev. A **28**, 1237 (1983); L. S. Cederbaum, in *Encyclopedia of Computational Chemistry*, edited by P. v. R. Schleyer, P. R. Schreiner, N. A. Allinger, T. Clark, J. Gasteiger, P. Kollman and H. F. Schaefer III (Wiley, New York, 1998).
[14] U. Fano, Phys. Rev. **124**, 1866 (1961).
[15] R. K. Nesbet, Phys. Rev. A **14**, 1065 (1976).
[16] V. V. Ivanov and A. V. Luzanov, J. Struct. Chem. **38**, 10 (1997).
[17] H. Ågren, V. Carravetta, H. J. Aa. Jensen, P. Jørgensen, and J. Olsen, Phys. Rev. A **47**, 3810 (1993).
[18] V. Carravetta, Yi Luo, and H. Ågren, Chem. Phys. **174**, 141 (1993).
[19] K. Gokhberg, V. Vysotskiy, L. S. Cederbaum, L. Storchi, F. Tarantelli, and V. Averbukh, J. Chem. Phys. **130**, 064104 (2009).
[20] B. N. Parlett, *The Symmetric Eigenvalue Problem* (Prentice-Hall, Englewood Cliffs, NJ, 1980).
[21] G. H. Golub and C. F. van Loan, *Matrix Computations* (The Johns Hopkins University Press, Baltimore, 1989).
[22] G. Howat, T. Åberg, and O. Goscinski, J. Phys. B **11**, 1575 (1978).
[23] G. Howat, J. Phys. B **11**, 1589 (1978).
[24] J. Schirmer, Phys. Rev. A **26**, 2395 (1982); F. Mertins and J. Schirmer, Phys. Rev. A **53**, 2140 (1996).
[25] J. Schirmer, Phys. Rev. A **43**, 4647 (1991).
[26] K. Andersson, M. Barysz, A. Bernhardsson, M. R. A. Blomberg, Y. Carissan, D. L. Cooper, M. P. Fülscher, C. de Graaf, B. A. Hess, D. Hagberg, G. Karlström, R. Lindh, P.-Å. Malmqvist, T. Nakajima, P. Neogrády, J. Olsen, J. Raab, B. O. Roos, U. Ryde, B. Schimmelpfennig, M. Schütz, L. Seijo, L. Serrano-Andrés, P. E. M. Siegbahn, J. Stålring, T. Thorsteinsson, V. Veryazov, and P.-O. Widmark, MOLCAS Version 6, Lund University, Sweden (2004).
[27] F. Müller-Plathe and G. H. F. Diercksen, in *Electronic Structure of Atoms, Molecules and Solids*, edited by S. Canuto, J. D'Albuquerque e Castro, and F. J. Paixão (World Scientific, Singapore, 1990).
[28] H.-D. Meyer and S. Pal, J. Chem. Phys. **91**, 6195 (1989).
[29] T. J. Park and J. C. Light, J. Chem. Phys. **85**, 5870 (1986).
[30] K. Schulz, M. Domcke, R. Püttner, A. Gutiérrez, G. Kaindl, G. Miecznik, and C. H. Greene, Phys. Rev. A **54**, 3095 (1996).
[31] L. Veseth, J. Phys. B **29**, 977 (1996).
[32] All standard Gaussian basis sets used in this work have been obtained from the EMSL Basis Set Library, D. Feller J. Comp. Chem. **17**, 1571 (1996); K. L. Schuchardt, B. T. Didier, T. Elsethagen, L. Sun, V. Gurumoorthi, J. Chase, J. Li, and T. L. Windus, J. Chem. Inf. Model. **47**, 1045 (2007).
[33] K. Kaufmann, W. Baumeister, and M. Jungen, J. Phys. B **22**, 2223 (1989).
[34] W. E. Davidson, J. Comput. Phys. **17**, 97 (1975).
[35] A. Y. Yencha, R. I. Hall, L. Avaldi, G. Dawber, A. G. McConkey, M. A. MacDonald, and G. C. King, Can. J. Chem. **82**, 1061 (2004).
[36] N. Moiseyev, Phys. Rep. **302**, 211 (1998).